Precipitation kinetics of calcite in the system CaCO3-H2O-CO2: The conversion to CO2 by the slow process H++HCO3-->CO2+H2O as a rate limiting step

Article *in* Geochimica et Cosmochimica Acta · September 1997

DOI: 10.1016/S0016-7037(97)00201-9

CITATIONS
127

READS
326

4 authors, including:

Dreybrodt Wolfgang
Universität Bremen
254 PUBLICATIONS **8,319** CITATIONS
SEE PROFILE

Laurent Paul Eisenlohr
Centro De Rehabilitación Física De Maldonado
36 PUBLICATIONS **725** CITATIONS
SEE PROFILE

Pergamon

Geochimica et Cosmochimica Acta, Vol. 61, No. 18, pp. 3897–3904, 1997

0016-7037/97 $17.00 + .00

PII S0016-7037(97)00201-9

Precipitation kinetics of calcite in the system $CaCO_3 - H_2O - CO_2$: The conversion to CO_2 by the slow process $H^+ + HCO_3^- \rightarrow CO_2 + H_2O$ as a rate limiting step

W. DREYBRODT, L. EISENLOHR, B. MADRY, and S. RINGER
Institute of Experimental Physics, University of Bremen, 28334 Bremen, Germany

(*Received December* 19, 1996; *accepted in revised form May* 21, 1997)

Abstract—Precipitation rates of $CaCO_3$ from supersaturated solutions in the $H_2O - CO_2 - CaCO_3$ system are controlled by three rate-determining processes: the kinetics of precipitation at the mineral surface, mass transport of the reaction species involved to and from the mineral surface, and the slow kinetics of the overall reaction $HCO_3^- + H^+ \rightarrow CO_2 + H_2O$. A theoretical model by Buhmann and Dreybrodt (1985a,b) taking these processes into account predicts that, due to the slow kinetics of this reaction, precipitation rates to the surface of $CaCO_3$ minerals depend critically on the ratio V/A of the volume V of the solution to the surface area A of the mineral in contact with it, for both laminar and turbulent flow. We have performed measurements of precipitation rates in a porous medium of sized particles of marble, limestone, and synthetic calcite, with V/A ratios ranging from $3 \cdot 10^{-4}$ to $1.2 \cdot 10^{-2}$ cm at 10°C. Calcite was precipitated from supersaturated solutions with $[Ca^{2+}] \approx 4$ mmol/L and an initial P_{CO_2} of $5 \cdot 10^{-3}$ or $1 \cdot 10^{-3}$ atm, respectively, using experimental conditions which prevented exchange of CO_2 with the atmosphere, i.e., closed system. The results are in qualitative agreement with the theoretical predictions. Agreement with the observed data, however, is obtained by modifying the rate law of Plummer et al. (1978) to take into account surface-controlled inhibition effects. Experiments with supersaturated solutions containing carbonic anhydrase, an enzyme which enhances the conversion of HCO_3^- into CO_2, yield rates increased by a factor of up to 15. This provides for the first time unambiguous experimental evidence that this reaction is rate limiting. We have also measured precipitation rates in batch experiments, stirring sized mineral particles in a solution with V/A ranging from 0.03 to 0.75 cm. These experiments also give clear evidence on the importance of the conversion of HCO_3^- into CO_2 as rate limiting step. Taken together our experiments provide evidence that the theoretical model of Buhmann and Dreybrodt (1985a,b) can be used to predict reliable rates from the composition of Ca^{++}-HCO_3^- solutions with low ionic strength in many geologically relevant situations.

1. INTRODUCTION

The kinetics of the precipitation of calcium carbonate is fundamental to understanding many natural geochemical systems. The evolution of the chemical composition of calcite-depositing stream systems depends critically on the kinetics of calcite precipitation (Dreybrodt et al., 1992; Liu et al., 1995). Calcite precipitation plays an important role in diagenesis (Boudreau and Canfield, 1993) of calcareous deep-sea sediments. Many tourist attractions, such as the sinter terraces of Pamukkale in Turkey, are endangered by pollutants, which inhibit further deposition of calcite and can lead to a decay of the beauty of such sceneries (Ekmekçi, 1995). Since the deposition of $CaCO_3$ from aqueous solution releases carbon dioxide it also plays an important role in the global cycle of CO_2 (Archer and Maier-Reimer, 1994). Speleothems such as stalagmites, stalactites, and flowstone contain significant information on paleoclimate (Baker et al., 1993, 1995; Shopov et al., 1994; Genty and Quinif, 1996). It is therefore of importance to understand the mechanisms of their growth (Dreybrodt, 1980, 1981, 1982, 1988; Baker and Smart, 1995; Ford et al., 1993).

To understand these processes numerous studies have been carried out to obtain experimental rates of calcium carbonate precipitation (Nancollas and Reddy, 1971; House, 1981; Reddy et al., 1981; Morse, 1983; Inskeep and Bloom, 1985; Busenberg and Plummer, 1986; Zhong and Mucci, 1993; Zuddas and Mucci, 1994; Shiraki and Brantley, 1995). Calcite precipitation mechanisms have also been investigated by Scanning Force Microscopy (Dove and Hochella, 1993; Gratz et al., 1993).

Most of these investigations aimed at deriving a rate equation, quantifying calcite precipitation rates in terms of the chemical composition of the solution at the mineral surface. The most widely accepted rate equation, the PWP equation (Plummer et al., 1978; Busenberg and Plummer, 1986) is believed to be valid for both precipitation and dissolution (Reddy et al., 1981; Shiraki and Brantley, 1995), provided the solution is sufficiently far from chemical equilibrium with respect to calcite. Close to equilibrium, inhibition processes are more effective and may prevent the solution from attaining equilibrium. The PWP equation reads

$$R = \kappa_1(H^+) + \kappa_2(H_2CO_3^*) + \kappa_3 - \kappa_4(HCO_3^-)(Ca^{2+}) \quad (1)$$

where κ_1, κ_2, κ_3, and κ_4 are rate constants and the parentheses denote activities. Using this equation as a flux boundary condition, Buhmann and Dreybrodt (1985a,b, 1987; Dreybrodt, 1988; Dreybrodt and Buhmann, 1991), developed a model which predicts dissolution or precipitation rates from water films covering a calcite surface, which are either stagnant, in laminar flow, or in turbulent motion. This model also considers mass transport to and from the mineral surface and the slow overall reaction $CO_2 + H_2O \leftrightarrow H^+ + HCO_3^-$.

This overall reaction has been described in detail by Kern (1960), Usdowski (1982), and Stumm and Morgan (1981). Reaction times for equilibrium with respect to CO_2 for waters of the type Ca^{2+}-Mg^{2+}-HCO_3^-, as they occur in limestone terrains, are on the order of 10s (Usdowski, 1982). This slow process will henceforth be termed conversion reaction.

An important result of the model of Buhmann and Dreybrodt is that at small ratios V/A, where V is the volume of the solution and A the area of the mineral surface, the rates are controlled by this slow reaction. This can be qualitatively explained by the following arguments. Since precipitation of calcite is determined by the overall reaction $Ca^{2+} + 2HCO_3^- \rightarrow CaCO_3 + H^+ + HCO_3^- \rightarrow CaCO_3 + CO_2 + H_2O$ stoichiometry requires that one molecule of CO_2 is released for each $CaCO_3$ deposited to the surface. Therefore, the following relation holds in any case:

$$V\frac{d[CO_2]}{dt} = AR \qquad (2)$$

where $[CO_2]$ is the concentration of CO_2. For sufficiently small V/A ratios the left-hand side of Eqn. 2, representing the amount of CO_2 released per time becomes rate limiting. At large V/A ratios, however, sufficient amounts of CO_2 are released and the rates are controlled by the surface reaction, represented by the right-hand side of Eqn. 2. In the case of $V/A < 0.1$ cm for stagnant, laminarly, or turbulently flowing solutions, the precipitation rates are drastically reduced compared to the predictions of the PWP equation. In the interpretation of calcite dissolution or precipitation in a $Ca^{2+} - HCO_3^-$ solution with low ionic strength this important role of CO_2 conversion has often been overlooked, and the PWP equations have been used uncritically. Buhmann and Dreybrodt (1985a) verified their theoretical results experimentally for precipitation from thin water layers of 0.01 cm covering marble samples as they occur in the growth of stalagmites. Later, Baker and Smart (1995) and Baker et al. (1996) successfully used the model to understand the growth rates of flowstone. In a recent paper, Dreybrodt et al. (1996) compared the theoretical predictions of the model to experimental data of dissolution rates in turbulently flowing solutions in batch experiments and stagnant solutions contained in porous media. They found satisfactory agreement with the theory. In this paper, we report similar experiments for values of V/A ranging from $3 \cdot 10^{-4}$ cm up to 0.75 cm to investigate precipitation rates.

These experiments give the first unambiguous evidence that the slow conversion reaction of HCO_3^- into CO_2 determines the rates in many geological situations, such as precipitation of calcite in porous media and narrow joints, and must not be overlooked.

2. THEORETICAL BACKGROUND

Precipitation of calcite from solutions containing $CaCO_3$ and CO_2 can occur under conditions where the system is either open or closed with respect to CO_2. In the first case, CO_2 can escape from the system by crossing a phase boundary between the solution and the atmosphere. If the surface area of the mineral grains to which calcite is deposited is much larger than the surface area of the phase boundary, the transfer of CO_2 across this boundary layer can be rate limiting (Arakaki and Mucci, 1995). Therefore, experiments investigating precipitation or dissolution rates of calcite in porous media with large surface areas should be performed under closed system conditions in order to avoid transfer of CO_2 out of the solution.

Buhmann and Dreybrodt (1985b) calculated precipitation rates as a function of the calcium concentration as it develops in a free-drift run of calcite precipitation from a supersaturated solution with defined initial P_{CO_2} contained between two parallel surfaces of calcite with distance 2δ, in either stagnant or laminar flow. Later, Baumann et al. (1985) showed that these results are also valid for a porous medium of average grain size $\bar{d}$. In this case Baumann et al. (1985) had to replace the width between the parallel surfaces on the idealised model by the average distance between two adjacent grains of the porous medium. For an average grain size, $\bar{d}$, this distance, $\bar{\delta}$, is given by $\bar{\delta} = 0.19\,\bar{d}$. It should be noted that for both cases—the idealised parallel fracture and the porous medium—the V/A ratio is related to the distance between the planes by $\delta = V/A$, and to the average distance, $\bar{\delta}$, in the porous medium, by $\bar{\delta} = V/A$, respectively. (Baumann et al., 1985).

In all these model calculations, transport equations were solved numerically. They contain the precipitation rates due to the PWP equation as a boundary condition of the flux at the mineral surface, mass transfer by molecular diffusion from and to the mineral surface, and the slow conversion reaction.

Results are shown in Fig. 1, where we present precipitation rates for porous media with various values of $\bar{d}$ used later in the experiments. The numbers on the curves indicate the values of $\bar{d}$. Each of the curves in Fig. 1 represents the precipitation rates in a free-drift run when a supersaturated solution brought to equilibrium with a P_{CO_2} of $5 \cdot 10^{-3}$ atm starts to lose Ca^{2+} in a closed system by precipitation of calcite and finally reaches equilibrium with respect to calcite.

At small V/A ratios, conversion of HCO_3^- to CO_2 be-

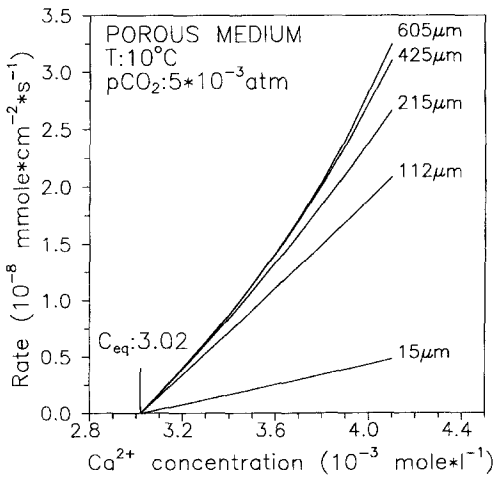

Fig. 1. Precipitation rates calculated from the model of Buhmann and Dreybrodt (1985b) for a porous medium for various grain sizes, $\bar{d}$, as given on the curves.

comes rate limiting. Therefore, the rates for $\bar{d} = 15$ μm are small. They increase with the increasing V/A ratio until they reach a limit where both mass transport and CO_2 conversion determine the rates (Buhmann and Dreybrodt, 1985a,b). It is most important to note that for grain sizes $\bar{d} < 4 \cdot 10^{-2}$ cm, corresponding to V/A $\leq 8 \cdot 10^{-3}$ cm, the precipitation rates depend strongly on $\bar{d}$.

In all the calculations above, the water film was assumed to be stagnant. If deposition occurs from a bulk solution which is in turbulent motion, mass transport by diffusion is enhanced by turbulent eddies. This can be simulated by increasing the constant of molecular diffusion by a factor of 10^4 (Buhmann and Dreybrodt, 1985a,b). The results for various values of V/A in this case are shown by Fig. 2. They are also valid for batch experiments, where particles of total surface area, A, are turbulently stirred in solution of volume, V. Because of the enhanced diffusion, concentration gradients cannot form. Therefore, in the case of turbulent motion, the deposition rates increase dramatically up to almost 10^{-6} mmol/cm^{2}s. They also depend strongly on the V/A ratio due to the influence of $HCO_3^- \rightarrow CO_2$ conversion.

It should be noted here that our model with turbulent motion is based on the assumption that the chemical composition of the solution at the surface of the carbonate mineral is identical with that of the bulk solution. This is not true when a laminar diffusion boundary layer exists between the bulk and the reacting surface. In this case, concentration gradients resulting from molecular diffusion through this layer change the concentrations at the mineral surface and the rates can be reduced depending on the thickness of the boundary layer down to about 10% of the maximal rate (Dreybrodt and Buhmann, 1991). Experimental verification may therefore deviate from this simple approach.

3. EXPERIMENTAL METHODS

3.1. Samples and sample preparation

Baker-analyzed reagent $CaCO_3$ was prepared by suspending it in bidistilled water to remove microparticles. The material was then treated for 10 s with dilute HCl and washed with bidistilled water and finally, with acetone. The material was stored after drying at 50°C for 5 h. A microscopic analysis revealed crystals of an average size of 15 μm, which yields a geometric surface area of 1740 cm^2/g, similar to the area of 1840 cm^2/g obtained by BET-measurements.

Natural marble (Naxos, Greece) and limestone (Swiss Jura) were broken down and sized by wet sieving with deionized water to fractions between 100 μm and 125 μm, 180 μm and 250 μm, 350 μm and 500 μm, and 500 μm and 710 μm. The samples were treated with dilute HCl (0.01 molar) for 10 s, rinsed in bidistilled water and finally, with acetone. We also prepared some samples without acetone wash and used these immediately. Within the limits of error they showed the same behaviour in the precipitation rates as those treated with acetone. They were then dried and stored for further use. Their surface area was determined from the geometrical surface area of rhombohedrons. The sized fraction from 100–125 μm had a surface of 312 cm^2/g. Accordingly, values of 163 cm^2/g, 82 cm^2/g, and 58 cm^2/g were obtained for the fractions 180–250 μm, 350–500 μm and 500–700 μm, respectively. These values were also found within an error of 10% by BET measurements. Carbonic anhydrase from bovine erythrocytes was purchased as lyophilized powder from Sigma Chemical Co. and was used as obtained.

Supersaturated solutions of $CaCO_3$ with Ca^{2+} concentrations several mmol above equilibrium were prepared by dissolving Baker calcite in thermostated bidistilled water of a given temperature through which CO_2 ($P_{CO_2} = 1$ atm) was bubbled until the desired

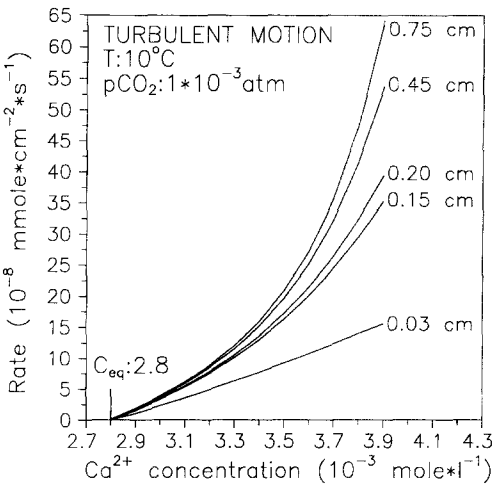

Fig. 2. Precipitation rates calculated from the model of Buhmann and Dreybrodt (1985b) for a solution in turbulent motion. The numbers on the curves denote the V/A ratios.

Ca^{2+} concentration was reached. This was monitored by measuring conductivity, as will be discussed in the next section. The solution was then filtered and pure nitrogen was bubbled through it to reduce the CO_2 concentration to the desired value so that the solution became supersaturated with respect to calcite. By means of the program Equilibrium, which calculates the chemical composition of the solution for an open system from the calcium-concentration and P_{CO_2} (Dreybrodt, 1988), we then obtained the pH value corresponding to the desired P_{CO_2} in the solution. During degassing of CO_2 from the solution, pH was monitored until this desired pH value was reached. We thus obtained solutions several mmol above equilibrium with respect to calcite. Before using the solution we again filtered it through micropore filters with 0.45 μm pore size. At the time the experiment was started, an aliquot of the solution was taken and the calcium concentration was determined by immediate titration using standard methods. The calcium concentration was analysed by EDTA titration with calcium indicator Cal/Ver® with an accuracy of ±3%.

3.2. Apparatus

The first experiment type was carried out in batch runs using the free-drift technique in which calcite particles were kept in suspension by vigorously stirring the solution with a Teflon propeller at 350 rpm. Figure 3 shows the experimental setup. The solution is contained in a Teflon vessel with a volume of 262 cm^3, and no further space is available for air. The vessel is sealed to be airtight. The experiment was started by filling the vessel with the supersaturated solution of $CaCO_3$ of defined initial partial pressure of CO_2. The temperature was kept at 10 ± 0.1°C. Immediately after filling, a defined amount of a sized fraction of marble or Baker calcite was introduced. The vessel was sealed by a stopper and the stirrer switched on. This experimental step was completed within 1 min. During the experimental runs the calcium concentration, c, was monitored by measuring the conductivity, σ, to an accuracy within ±1%. The linear relation between c and σ was determined in the following way. First we calculated the chemical composition of the solution at equilibrium with a CO_2 atm of $5 \cdot 10^{-3}$ and $1 \cdot 10^{-3}$, as it develops in a free-drift run under closed system conditions for various values of Ca^{2+} concentrations, c. This was done using the program Equilibrium (Dreybrodt, 1988). Thus we obtained pH, $[HCO_3^-]$, and $[CO_3^{2-}]$ as a function of c. These values were then used to calculate the conductivity by using WATEQ.4F. In the region of our experimental conditions we found the relation:

$$c = 6.07 \cdot 10^{-3} \cdot \sigma - 0.3 \qquad (3)$$

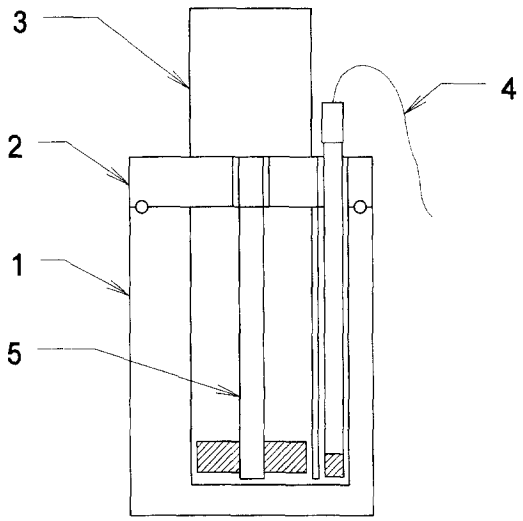

Fig. 3. Experimental setup for a batch run. A vessel of Teflon (1) is sealed by a lid (2). The lid carries a motor (3). Its shaft (5), also covered by Teflon, is sealed with respect to the atmosphere. The conductance is measured by the conductivity cell (5). The lid is also provided with a port for filling the vessel (not shown).

to be valid within ±1%, where c is in mmol/L and σ in μs/cm. This is in agreement with the empirical relation found by Langmuir (1971) for pure carbonate groundwaters.

The initial calcium concentration of the solution was measured by standard titration and used for calibration. The precipitation rates were then calculated from

$$-\frac{V}{A}\frac{dc(t)}{dt} = R \qquad (4)$$

Note that under our experimental conditions the surface onto which calcite is deposited does not change by more than 3% for batch experiments and by 0.03% for the porous medium. Before differentiation, the experimental time variation, $c(t)$, of the concentration was fitted to the expression

$$c(t) = A_0 e^{-t/A_1} + A_2 + A_3 t + A_4 t^2 + A_5 t^3 + A_6 t^4 \qquad (5)$$

where A_0, A_1, A_2, A_3, A_4, A_5, and A_6 are fitting constants. We obtained excellent fits with correlation coefficients of $r^2 = 0.999$ and residuals of less than 2%. This procedure avoids excessive noise resulting from numerical differentiation of the original data points and thus resembles an effective smoothing of the data.

The second experiment type of employed precipitation of calcite in a porous medium which contained a stagnant solution contained. The experimental setup is shown in Fig. 4. The upper drawing represents a longitudinal section of the setup. A WTW-conductivity cell (Tetracon LF 325) (1), also shown in top view below, is surrounded by a cooling vessel (5) to keep the temperature constant to ±0.1°C. The electrodes (4) of the cell are located at the walls of a slit which is 3 cm long and 0.6 cm wide. This slit is filled with 3 g of sized calcite (3). To start the experiment, 2 cm^3 of the supersaturated solution are poured into the calcite medium, and air bubbles in the porous medium are removed by stirring for a second. The porous medium is covered with an airtight lid (2) to ensure closed system conditions. This procedure takes less than 10 s. To obtain precipitation rates, the same electrode is used to measure the decrease in conductivity. Each experiment was carried out 3 times. The results were reproduced within an error of 10%. To estimate the V/A ratio from the average particle size, we assume the particles to be rhombohedra with diameter, $\bar{d}$, of its largest surface diagonal. Thus one obtains $V/A = 0.19 \cdot \bar{d}$. To ensure that the device was closed with respect to CO_2, a solution of CO_2 in distilled water with $P_{CO_2} = 1$ atm was introduced into the empty cell. It was then sealed and the

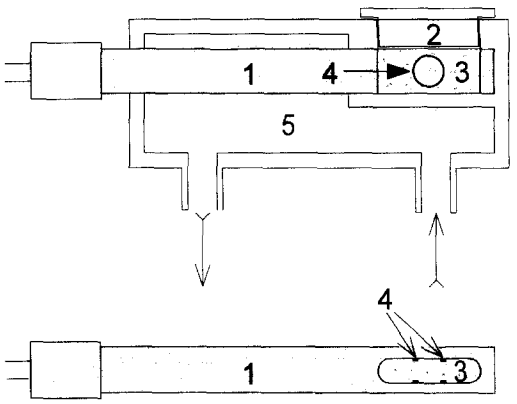

Fig. 4. Upper drawing: Experimental setup for the experiments with porous media: The conductivity cell (1) is surrounded by a cooling vessel (5) using thermostated water. The space (3) between the electrodes (4) is filled with sized calcite grains. After filling this space with supersaturated solution, the setup is sealed by the lid (2). Lower drawing: The WTW cell (1) showing the space between the electrodes in top view.

conductivity of the solution was measured. Observation of a constant conductivity within ±0.5% during a period of 2 days indicated that the maximal relative loss of CO_2 was less than $2.8 \cdot 10^{-5}$%.

4. EXPERIMENTAL RESULTS

Figure 5 depicts the time variation c(t) of the Ca^{2+} concentration and the fits using Eqn. 4 (solid lines) for the batch experiment with turbulent motion of the solution. The numbers on the curves refer to the V/A ratio. The rates obtained from differentiating the fit expressions (Eqn. 5) from such experiments are depicted in Fig. 6. The solid lines show the precipitation rates of Baker calcite with various V/A ratios given by the numbers on the curves. The theoretically predicted dependence of the rates on the V/A ratios

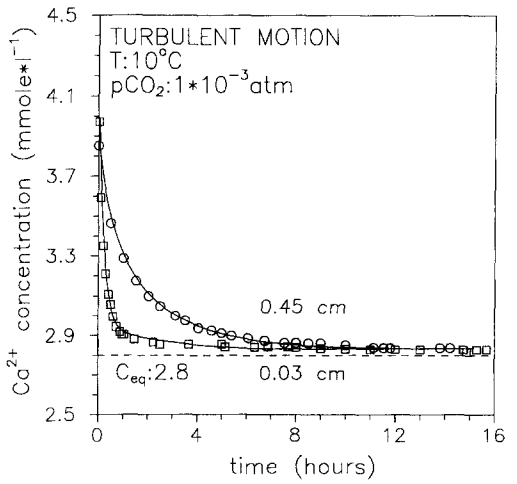

Fig. 5. Decrease of calcium concentration, $c(t)$, during precipitation of calcite to particles from a solution in turbulent motion. The numbers on the curves denote V/A, the ratio of the volume, V, of the solution to the total surface area, A, of the particles. The solid line represents the fit by Eqn. 5 through the data points.

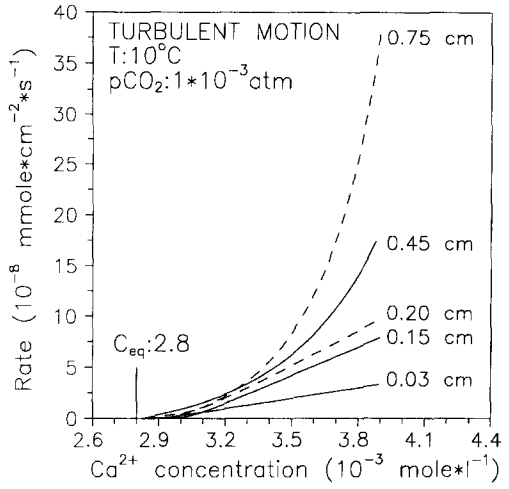

Fig. 6. Precipitation rates as a function of calcium concentration in the batch experiment from time variation, $c(t)$, as shown by Fig. 5. The solid lines show experiments using Baker calcite, whereas the dotted lines depict runs with marble ($\bar{d}$ = 112 μm). The numbers on the curves denote the V/A ratio.

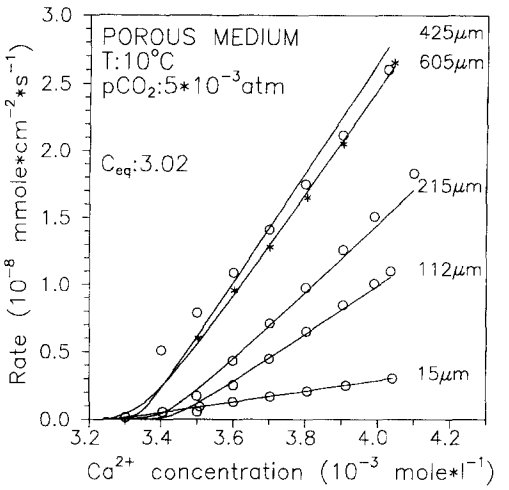

Fig. 8. Precipitation rates as a function of Ca concentration in a porous medium experiment from time courses, $c(t)$, as shown in Fig. 7. The numbers on the curves denote the average grain size, $\bar{d}$. The curves approach an apparent equilibrium at about 3.3 mmol/L. The theoretical predictions using the modified PWP equation (Eqn. 6) are shown by open circles and stars (425 μm).

(see Fig. 2) is qualitatively well seen. Closer inspection, however, reveals that the experimental rates are too low, especially close to equilibrium. The dotted lines illustrate experiments where marble with an average size $\bar{d}$ = 112 μm was used. These show analogous results.

The time variation of the concentration for the second type of experiments employing porous media is shown by Fig. 7 for two grain sizes. The solid lines represent the fits to the data points. After a steep decrease, the Ca^{2+} concentration slowly approaches a quasi-equilibrium far from the chemical equilibrium, depicted by the dotted line. This slow quasi-linear decrease was observed in long-term runs to persist for times up to several days, without reaching chemical equilibrium.

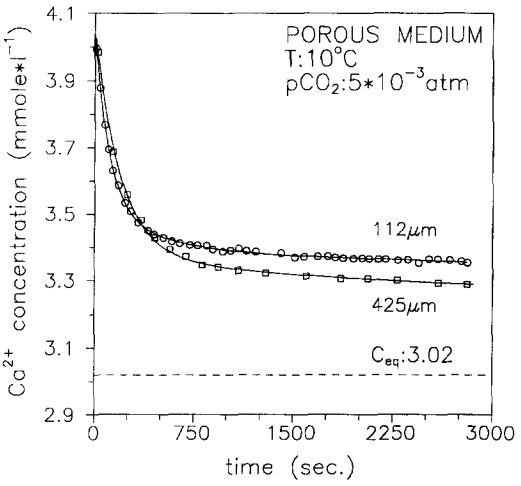

Fig. 7. Decrease of calcium concentration, $c(t)$, during precipitation of calcite in a porous medium. The solid lines represent the fits according to Eqn. 5. Two experiments with $\bar{d}$ = 112 μm and $\bar{d}$ = 425 μm are shown.

The rates obtained from such runs are plotted in Fig. 8. The curves initially show a linear reduction of the rates with respect to $[Ca^{2+}]$, but then at about 3.3 mmol/L they bend to very low rates far from equilibrium at 3.02 mmol/L. Inhibition of precipitation thus becomes apparent. Furthermore, the observed rates, although they resemble the theoretical predictions (Fig. 1), are qualitatively too low. The dependence of the experimentally observed rates on the V/A ratio, however, gives clear evidence of the rate-limiting role of the slow conversion reaction $HCO_3^- + H^+ \rightarrow H_2O + CO_2$. We have also performed these experiments with an initial calcium concentration of 3.8 mmol/L and $P_{CO_2} = 5 \cdot 10^{-3}$ atm, and also 4.2 mmol/L with initial P_{CO_2} of $1 \cdot 10^{-3}$ atm. The results, not shown here, are similar. The values of $\Omega = IAP/K_c$, where IAP is the ion-activity product of Ca^{2+} and CO_3^{2-} and K_c is the calcite solubility product with respect to calcite, covered the region from $1.5 \geq \Omega \geq 68$. Further experiments have been performed using limestone (Swiss, Jura), which also exhibited analogous behaviour.

To give additional evidence for the importance of the conversion reaction of HCO_3^- into CO_2 we have used supersaturated solutions of $CaCO_3$ containing the enzyme carbonic anhydrase (CA) at two concentrations, 0.067 μmol/L and 0.67 μmol/L, respectively. This enzyme enhances the conversion reaction dramatically (Lindskog et al., 1971; Stryer, 1988) and we have recently used it (Dreybrodt et al., 1996) to enhance dissolution rates in a similar experiment. From the Michaelis-Menten equation, the accelerated rate constant of CO_2 conversion $K^{acc}_{CO_2}$ is obtained (Stryer, 1988) by $K^{acc}_{CO_2} = k_e \cdot [E]/(K_m + [CO_2])$, where k_e is the turnover number of the enzyme and K_m the Michaelis constant. Their values are $k_e = 6 \cdot 10^5 s^{-1}$ and $K_m = 8 \cdot 10^{-3}$ mol/L at 25°C. We performed the experiment at 10°C and with initial $p_{CO_2} = 5 \cdot 10^{-3}$ atm. In this run, the CO_2 concentration increases from initially $1.6 \cdot 10^{-4}$ mol/L to $8 \cdot 10^{-4}$ mol/L

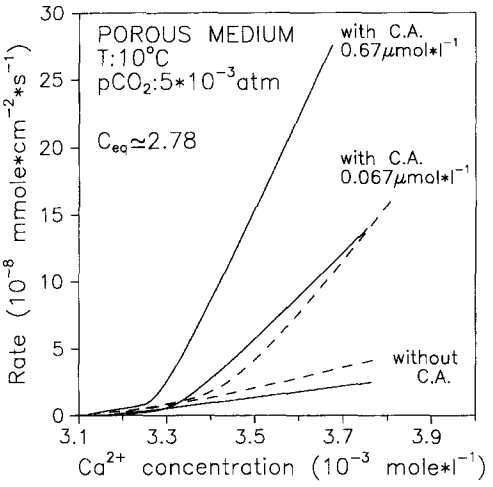

Fig. 9. Precipitation rates as a function of Ca concentration in a porous medium experiment from supersaturated solutions in the presence and absence of carbonic anhydrase. The solid lines denote experiments with $\bar{d}$ = 425 μm, the dashed lines denote experiments with $\bar{d}$ = 605 μm. Note that at calcium concentrations of about 3.3 mmol/L the curves bend, indicating a switch to inhibition region B (see text).

when equilibrium with respect to calcite is achieved in the closed system. Therefore, $[CO_2]$ in the denominator of the above equation can be safely neglected. With $[E]$ = 0.67 μmol/L we obtain $K^{acc}_{CO_2}$ = 50 s^{-1}, which, when compared to the value K_{CO_2} = 0.03 s^{-1}, is larger by a factor of 1666. Since in a catalysed reaction equilibrium is not shifted, the backward reaction $HCO_3^- + H^+ \rightarrow H_2O + CO_2$ is also enhanced by this factor.

If the conversion reaction is accelerated sufficiently, it should no longer be rate limiting and therefore the presence of CA should enhance the precipitation rates. Figure 9 illustrates that this is the case. The solid lines represent the precipitation rates from a porous medium experiment with marble ($\bar{d}$ = 425 μm). The lowest of these is obtained using a supersaturated solution without CA. The two upper solid lines represent precipitation rates under the same experimental conditions in the presence of CA to the supersaturated solutions at concentrations of 0.067 μmol/L and 0.67 μmol/L, respectively. The dashed curves show the results of experiments with $\bar{d}$ = 605 μm without CA and with 0.067 μmol/L CA. For calcium concentrations above 3.3 mmol/L a significant increase of the rates is visible, but at lower concentrations, the curves bend and the influence of CA becomes negligible. This shows that close to equilibrium (C_{eq} = 3.02 mmol/L), surface reactions become rate limiting and also indicates inhibition of these reactions.

5. DISCUSSION

Comparison of the experimental data obtained from the batch experiments with turbulent motion with the theoretical predictions (cf. Fig. 2 and Fig. 6) reveals qualitative agreement. The experimental rates, however, are too low. In turbulent flow the hydrodynamic conditions in such experiments, however, are not well defined. Laminar boundary layers separating the surface of the particles from the turbulent core provide additional diffusional resistance to the flux of dissolved ions into the solution, and rates are reduced. Dreybrodt and Buhmann (1991) have extended their model to include such boundary layers. Since the thickness of these boundary layers, however, cannot be determined in batch experiments, this model cannot be applied. The experimentally observed reduction of the rates, however, is in agreement with the assumption that such boundary layers are present in the batch experiments.

We therefore restrict our further discussion to the porous media experiments where in contrast to the batch experiments, such complications due to hydrodynamics cannot arise. Although there is qualitative agreement between the experimental results and the theoretical predictions (cf. Figs. 1 and 8), quantitatively, there are deviations. As predicted by the model, the initial rates depend critically on the pore size of the medium, indicating the importance of the conversion reaction. The relative magnitudes for various $\bar{d}$, however, deviate significantly. Furthermore, the observed rates are too low by a factor of roughly 2. Finally, they become extremely low at concentrations still far distant from equilibrium, with Ω close to 2. Below this value precipitation is strongly inhibited. After a first steep decrease of the concentration, there is a further lengthy, slow decrease, and the system slowly approaches equilibrium. A similar inhibition behaviour has been observed by Burton and Walter (1990), Mucci (1986), and Reddy (1977) for inhibitors such as phosphate. Thus, two regions of inhibition seem to be apparent. In region A, far from equilibrium, the rates are reduced moderately by approximately a factor of 2 until a quasi-equilibrium is reached.

From thereon (region B), a further reduction of the rates becomes operative, as is shown by the bending of the curves. This is seen especially well in the experiments using carbonic anhydrase (cf. Fig. 9). In this case the influence of the surface controlled reaction is dominant and its reduction close to quasi-equilibrium is clearly marked in Fig. 9. The reason of this inhibition is not clear, since no inhibiting ions, such as phosphate, were contained in the solution.

To describe the behaviour of the precipitation rates in region A, we modify the PWP equation in the following way:

$$R = \kappa_1(H^+) + \kappa_2(H_2CO_3^*) + \kappa_3 - f\cdot\kappa_4(Ca^{2+})(HCO_3^-) \quad (6)$$

where $f < 1$ is a factor which reduces the rates of the backward reactions and thus simulates inhibition. By this modification, the new apparent equilibrium is shifted to higher Ca^{2+} concentrations, since the forward reaction is dominated by κ_3, which is independent of the chemical composition of the solution. Calculations of the chemical composition of our solutions by Equilibrium and WATEQ4F have shown that ion pairs can be neglected, and also that for our experimental conditions, $[Ca^{2+}] = 2[HCO_3^-]$. Assuming that the inhibited rates become zero at $[Ca^{2+}]_{app}$ from Eqn. 6, we find $\kappa_3 = f\cdot\kappa_4[Ca^{2+}]^2_{app}$. On the other hand, from Eqn. 1, true equilibrium is found as $\kappa_3 = \kappa_4[Ca^{2+}]_{eq}$. Therefore:

$$f = \left(\frac{[Ca^{2+}]_{eq}}{[Ca^{2+}]_{app}} \right)^2 \quad (7)$$

where $[Ca^{2+}]_{eq}$ is the true chemical equilibrium and $[Ca^{2+}]_{app}$ is the apparent quasi-equilibrium, limiting inhibition region B. Modifying our theoretical model by Eqn. 6, we then adjusted f in such a way that the experimentally observed rates were obtained. Table 1 lists these estimated values of f for the experiments using Baker calcite, marble, and limestone for various $\bar{d}$ and a P_{CO_2} of $5 \cdot 10^{-3}$ atm or $1 \cdot 10^{-3}$ atm. It turns out that all values obtained are constant within an error of ±15%. For both marble and limestone, the average value of $f = 0.7 \pm 0.1$. In the case of Baker calcite, f values with $f = 0.7 \pm 0.02$ result. Thus the modification of the model allows for prediction within inhibition region A of all experimentally observed rates with a precision of about 10% with only *one* fitting parameter, f. This is illustrated by the open circles in Fig. 8, which represent the rates as calculated from the theoretical model using Eqn. 6. The stars belong to the experiment with 425 μm. The values of f are the average values listed in Table 1. This is an entirely empirical treatment, which does not elucidate the reason for the inhibition which is present in both natural and synthetic materials.

Nevertheless, a few comments should be given. It is interesting to note that inhibition region A covers saturation states with $\Omega > 2$ in all our experiments, whereas values with $\Omega < 2$ are characteristic for region B. This is in accordance with the observations of Busenberg and Plummer (1986), who found two regions of precipitation. Region I, covered by solutions with $1 < \Omega < 1.5$, shows extremely low rates of precipitation, whereas region II, with $\Omega > 1.5$, exhibits growth rates, following a rate law

$$R = \kappa_4 (C \cdot E - (Ca^{2+})(HCO_3^-)) \quad (8)$$

where C is a constant and E is the product of Ca^{2+} and HCO_3^- activities at equilibrium. This law turned out to be valid in the region $1.5 > \Omega > 100$. From Eqns. 7 and 8, one finds $C = 1/f$. Therefore, this is very similar to the modification of the PWP law in Eqn. 7. The difference is that $C > 1$ reflects an enhancement of the forward reaction, rather than an inhibition of the backward reaction as our treatment implies. But formally, Eqn. 8 is equivalent to Eqn. 6.

Table 1. Inhibition factor f for various experiments with porous media.

Experiment	f
$P_{CO_2} = 5 \cdot 10^{-3}$ atm	
Baker, 15 μm	0.72 ± 0.02
marble, 112 μm	0.54 ± 0.05
marble, 215 μm	0.6 ± 0.05
marble, 425 μm	0.77 ± 0.08
marble, 602 μm	0.72 ± 0.07
limestone, 40 μm	0.54 ± 0.05
limestone, 150 μm	0.65 ± 0.07
limestone, 602 μm	0.74 ± 0.02
$P_{CO_2} = 1 \cdot 10^{-3}$ atm	
marble, 112 μm	0.67 ± 0.06
marble, 215 μm	0.62 ± 0.06

Recent experiments using scanning force microscopy on synthetic calcite crystals exposed to super-saturated solutions (Dove and Hochella, 1993) have revealed that precipitation regions I and II exhibit different mechanisms in growth. Growth in region II is determined by the formation of surface nuclei, which spread, coalesce, and continue growing. Addition of phosphate inhibits these processes. Since we use natural material, it is likely that impurities located at the mineral surface also play an inhibiting role, thus reducing the effective surface where the nucleation can take place. The influence of such inhibitors was recently observed (Svensson and Dreybrodt, 1992) for dissolution rates on marble and limestone samples. Growth rates in region I have low sensitivity to the saturation state and surface nucleation appears to be relatively unimportant. Our measurement of long time runs in this region reveals an almost constant rate, with a small linear decrease in time. At a calcium concentration of 3.1 mmol/L, rates of about $6 \cdot 10^{-11}$ mmol/cm^{2}s were observed. At the present state, our treatment aims are to develop a plausible explanation of the reduction of the observed rates. Futher work is necessary to explain the origin of the inhibition.

6. CONCLUSION

The results of this study demonstrate that precipitation rates of calcite are dependent on the geometrical structure of the geological environment. Due to the influence of the slow reaction $H^+ + HCO_3^- \rightarrow H_2O + CO_2$, the rates are determined by the ratio of the solution volume to the mineral surface area. Thus, for very fine grained carbonate sediments in contact with stagnant or laminarly flowing solutions with $V/A \approx 10^{-4}$ cm, rates can be reduced by two orders of magnitude from the maximal possible values determined by the PWP equation. Even for grain sizes of about 1000 μm, rates are still reduced by one order of magnitude.

Our findings emphasize the importance of considering the geometric conditions in all geological systems where estimates of precipitation rates are needed. The same holds when precipitation occurs in small fractures with openings between 10 μm and 1000 μm in both laminar and turbulent flow. Our experiments show further that for solutions with $\Omega > 2$, the rates can be reliably predicted by modifying the PWP equation in such a way that the back reactions causing precipitation are reduced by a factor of ≈0.7 for natural materials. Taken together, these results and those previously reported for dissolution (Dreybrodt et al., 1996) give clear evidence that the model of Buhmann and Dreybrodt (1985a,b) can be used reliably to predict rates in those regions, where the PWP rate equation or its modified versions are valid.

Acknowledgments—We thank the Deutsche Forschungsgemeinschaft for financial support. L. Eisenlohr was supported by a grant from the National Swiss Foundation for Research.

REFERENCES

Arakaki T. and Mucci A. (1995) A continuous and mechanistic representation of calcite reaction-controlled kinetics in dilute solu-

tions at 25°C and 1 atm total pressure. *Aquatic Geochem.* **1,** 105–130.

Archer D. and Maier-Reimer E. (1994) Effect of deep-sea sedimentary calcite preservation on atmospheric CO_2 concentration. *Nature* **367,** 260.

Baker A. and Smart P. L. (1995) Recent flowstone growth rates: Field measurements in comparison to theoretical prediction. *Chem. Geol.* **122,** 121–128.

Baker A., Smart P. L., Edwards R. L., and Richards D. A. (1993) Annual growth banding in a cave stalagmite. *Nature* **364,** 518–520.

Baker A., Smart P. L., Barnes W. L., Edwards R. L., and Farrant A. (1995) The Hekla 3 volcanic eruption recorded in a Scottish speleothem? *The Holocene,* **5,** 336–342.

Baker A., Genty D., and Barnes W. L. (1996) Recent stalagmite growth rates: Cave measurements, theoretical predictions and the invironmental record. In *Climate Change: The Karst Record; Spec. Publ.* **Z,** pp. 7–9. Karst Waters Institute.

Baumann J., Buhmann D., Dreybrodt W., and Schulz W. (1985) Calcite dissolution kinetics in porous media. *Chem. Geol.* **53,** 219–228.

Boudreau B. P. and Canfield D. (1993) A comparison of closed- and open-system models for porewater pH and calcite-saturation state. *Geochim. Cosmochim. Acta* **57,** 317–334.

Buhmann D. and Dreybrodt W. (1985a) The kinetics of calcite dissolution and precipitation in geologically relevant situations of karst areas: 1. Open system. *Chem. Geol.* **48,** 189–1211.

Buhmann D. and Dreybrodt W. (1985b) The kinetics of calcite dissolution and precipitation in geologically relevant situations of karst areas: 2. Closed system. *Chem. Geol.* **53,** 109–124.

Buhmann D. and Dreybrodt W. (1987) Calcite dissolution kinetics in the system H_2O-CO_2-$CaCO_3$ with participation of foreign ions. *Chem. Geol.* **64,** 89–102.

Burton E. A. and Walter L. M. (1990) The effects of P_{CO_2} and temperature on magnesium incorporation in calcite seawater and $MgCl_2$-$CaCl_2$ solutions. *Geochim. Cosmochim. Acta* **55,** 777–785.

Busenberg E. and Plummer L. N. (1986) A comparative study of the dissolution and crystal growth kinetics of calcite and aragonite. In *Studies in Diagenesis* (ed. F. A. Mumpton); *U.S. Geological Survey Bulletin* **1578,** 139–168.

Dove P. M. and Hochella M. F., Jr. (1993) Calcite precipitation mechanisms and inhibition by orthophosphate: In situ observations by scanning force microscopy. *Geochim. Cosmochim. Acta* **57,** 705–714.

Dreybrodt W. (1980) Deposition of calcite from thin films of natural calcareous solutions and the growth of speleothems. *Chem. Geol.* **29,** 89–105.

Dreybrodt W. (1981) The kinetics of calcite precipitation from thin films of calcarous solutions and the growth of speleothems: Revisited. *Chem. Geol.* **32,** 237–245.

Dreybrodt W. (1982) A possible mechanism for growth of calcite speleothems without participation of biogenic carbon dioxide. *Earth Planet. Sci. Lett.* **58,** 239–299.

Dreybrodt W. (1988) *Processes in karst systems—Physics, chemistry and geology;* Springer Series in Physical Environments, Vol. 5. Springer.

Dreybrodt W. and Buhmann D. (1991) A mass transfer model for dissolution and precipitation of calcite from solutions in turbulent motion. *Chem. Geol.* **90,** 107–122.

Dreybrodt W., Buhmann D., Michaelis J., and Usdowski E. (1992) Geochemically controlled calcite precipitation by CO_2 outgassing: Field measurements of precipitation rates in comparison to theoretical predictions. *Chem. Geol.* **97,** 285–294.

Dreybrodt W., Lauckner J., Zaihua Liu, Svensson U., and Buhmann D. (1996) The kinetics of the reaction $CO_2 + H_2O \rightarrow H^+ + HCO_3^-$ as one of the rate limiting steps for the dissolution of calcite in the system H_2O-CO_2-$CaCO_3$. *Geochim. Cosmochim. Acta* **60,** 3375–3381.

Ekmekçi M. (1995) Guide Book Intern. Symposium and Field Seminar on Karst Waters & Environmental Impacts, Beldibi-Antalya-Turkey.

Ford D. C., Lundberg J., Palmer A. N., Palmer M. V., Dreybrodt W., and Schwarcz H. P. (1993) Uranium-series dating of the draining of an aquifer: The example of Wind Cave, Black Hills, South Dakota. *Geol. Soc. Amer. Bull.* **105,** 241–250.

Genty D. and Quinif Y. (1996) Annually laminated sequences in the internal structure of some Belgian stalagmites—Importance for paleoclimatology. *J. Sediment. Res.* **66,** 275–288.

Gratz A. J., Hillner P. E., and Hansma P. K. (1993) Step dynamics and spiral growth on calcite. *Geochim. Cosmochim. Acta* **57,** 491–495.

House W. A. (1981) Kinetics of crystallisation of calcite from calcium bicarbonate solutions. *J. Chem. Soc. Faraday Trans.* **77,** 341–359.

Inskeep W. S. and Bloom P. R. (1985) An evaluation of rate equations for calcite precipitation at p less than 0.01 atm and pH greater than 8. *Geochim. Cosmochim. Acta* **49,** 2165–2180.

Kern D. M. (1960) The hydration of carbon dioxide. *J. Chem. Educ.* **37,** 14–23.

Langmuir D. (1971) The geochemistry of some carbonate ground waters in Central Pennsylvania. *Geochim. Cosmochim. Acta* **35,** 1023–1045.

Linskog S., Henderson L. E., Kannan K. K., Liljas A., Nyman P. O., and Strandberg B. (1971) Carbonic anhydrase. In *The Enzymes,* Vol. 5 (ed. Paul D. Boyer). Academic Press.

Liu Z., Svensson U., Dreybrodt W., Daoxian Y., and Buhmann D. (1995) Hydrodynamic control of inorganic calcite precipitation in Huanglong Ravine, China: Field measurements and theoretical prediction of deposition rates. *Geochim. Cosmochim. Acta* **59,** 3087–3097.

Morse J. W. (1983) The kinetics of calcium carbonate dissolution and precipitation. In *Carbonates: Mineralogy and Chemistry* (ed. R. I. Reeder); *Rev. Mineral.* **11,** 227–264.

Mucci A. (1986) Growth kinetics and composition of magnesian calcite overgrowths precipitated from seawater: Quantitative influence of orthophosphate ions. *Geochim. Cosmochim. Acta* **50,** 2255–2265.

Nancollas G. H. and Reddy M. M. (1971) The crystallization of calcium carbonate II: Calcite growth mechanism. *J. Coll. Interface Sci* **37,** 824–930.

Plummer L. N., Wigley T. L. M., and Parkhurst D. L. (1978) The kinetics of calcite dissolution in CO_2-water systems at 5 to 60°C and 0.0 to 1.0 atm. CO_2, *Amer. J. Sci.* **278,** 537–573.

Reddy M. M. (1977) Crystallization of calcium carbonate in the presence of trace concentrations of phosphorus containing anions. *J. Crystal Growth* **41,** 287–295.

Reddy M. M., Plummer L. N., and Busenberg E. (1981) Crystal growth of calcite from bicarbonate solutions at constant pH and 25°C: A test of calcite dissolution model. *Geochim. Cosmochim. Acta* **45,** 785–794.

Shiraki R. and Brantley S. L. (1995) Kinetics of near-equilibrium calcite precipitation at 100°C: An evaluation of elementary reaction-based and affinity-based rate laws. *Geochim. Cosmochim. Acta* **59,** 1457–1471.

Shopov Y. Y., Ford D. C., and Schwarcz H. P. (1994) Luminescent microbanding in speleothems: High resolution chronology and paleoclimate. *Geology* **22,** 407–410.

Stryer L. (1988) *Biochemistry.* W. H. Freeman.

Stumm W. and Morgan J. J. (1981) *Aquatic Chemistry.* Wiley.

Svensson U. and Dreybrodt W. (1992) Dissolution kinetics of natural calcite minerals in CO_2-water systems approaching calcite equilibrium. *Chem. Geol.* **100,** 129–145.

Usdowski E. (1982) Reactions and equilibria in the systems CO_2-H_2O and $CaCO_3$-CO_2-H_2O. A review. *Neues Jahrb. Mineral. Abh.* **144,** 148–171.

Zhong S. and Mucci A. (1993) Calcite precipitation in seawater using a constant addition technique: A new overall reaction kinetic expression. *Geochim. Cosmochim. Acta* **57,** 1409–1417.

Zuddas P. and Mucci A. (1994) Kinetics of calcite precipitation from seawater. I. A classical chemical kinetics description for strong electrolyte solutions. *Geochim. Cosmochim. Acta* **58,** 4353–4362.